The PROBA/CHRIS Mission: A Low-Cost Smallsat for Hyperspectral, Multi-Angle, Observations of the Earth Surface and Atmosphere

M.J. Barnsley, J.J. Settle, M.A. Cutter, D.R. Lobb, F. Teston

Abstract— **The European Space Agency's Project for On-Board Autonomy is intended to demonstrate a range of innovations in the design, construction and operation of small satellites. It carries a number of scientific instruments, the most advanced of which is the Compact High-Resolution Imaging Spectrometer. A typical nadir image is $13km \times 13km$ in size and has 18 narrow spectral channels at $17m$ spatial resolution. When operated at $34m$ spatial resolution, the instrument can capture data in 62, almost contiguous, spectral channels. The platform is highly manoeuvrable: along-track pointing allows a given site to be imaged five times during a single overpass, while across-track pointing ensures that the revisit time for a site of interest is less than a week. This unique combination of spectral and angular sampling provides a rich source of data with which to study environmental processes in the atmosphere and at Earth's surface.**

I. Introduction

The Project for On-Board Autonomy (PROBA-1) satellite was launched from Shriharikota, India on 22 October 2001. Developed and built by a consortium led by the Belgian company Verhaert, and funded by the European Space Agency (ESA), PROBA-1 was originally intended to be a short, experimental, mission. Its primary objective was to test a number of innovations in platform design, principally relating to attitude control and recovery from errors, which would enable it to operate autonomously; that is, with the minimum amount of intervention from the ground. PROBA-1 carries on board a small number of scientific instruments, intended to demonstrate the use of the platform for both space and environmental studies. These include a sensor for detecting space debris, a space radiation-environment monitor and two digital cameras. The principal scientific instrument on board PROBA-1, however, is the Compact High Resolution Imaging Spectrometer (CHRIS). This sensor acquires high spatial resolution (17–20*m* or 34–40*m*) images of Earth's surface in up to 62 narrow spectral channels located in the visible and near infra-red wavelengths.

In addition to their respective scientific and technological objectives, the combination of CHRIS and PROBA is intended to serve as a demonstration of a faster approach to the design, launch and operation of scientific satellite-sensor missions. In this context, 'faster' refers to the relatively short time-period (two to three years) between the selection of CHRIS as the Announcement of Opportunity (AO) instrument and the launch of the PROBA platform. One of most significant benefits of this approach is the potential for greater responsiveness to the current and future needs of scientific users.

A novel feature of the PROBA-1 platform is that it can be manoeuvred in orbit using a set of four reaction wheels. These allow the satellite to be pointed off-nadir in both the along-track and across-track directions. This agility confers a number of obvious benefits. First, it increases the area of Earth's surface that is potentially visible to the on-board imaging instruments during a single orbit. Second, it allows the instruments to acquire images of cloud-free areas of Earth's surface at the expense of cloud-covered ones, and to avoid sun glint over water bodies. Third, by slowly pitching during image acquisition (i.e. through motion compensation), it is possible to improve the signal-to-noise performance by increasing the integration times. Finally, it provides a means by which images can be recorded at different sensor view angles. The latter is, of course, important for studies of the bidirectional reflectance properties of Earth's surface, and can also be used to generate digital elevation models through stereo photogrammetric reconstruction. In fact, PROBA-1 can be pitched sufficiently quickly along-track so that five separate CHRIS images can be obtained for a given target area during a single orbital overpass, with each image recorded at a different sensor view angle. This multiple-view-angle (MVA) imaging capability [1], in conjunction with the high spectral and spatial resolution of CHRIS, provides an enormously rich source of data for the scientific investigation of Earth's surface and atmosphere. Indeed, ESA has recognised the importance of such data to the characterisation of a range of environmental processes operating at the land surface, and have plans for a similar mission (SPECTRA), albeit on a much grander scale and over a longer period, to be launched later this decade. The lessons learned from the PROBA/CHRIS mission will be invaluable in helping to guide the development of this, more ambitious, programme.

II. The PROBA Platform

A. Overview

The primary purpose of the PROBA platform is to act as 'proof-of-concept' for a novel spacecraft technology. More specifically, it is intended to show the utility of on-board systems that may be used to control the satellite, including its general operation and the management of resources, spacecraft attitude, data communications and payload operations. The operation of the star trackers, on-board autonomy software and spacecraft attitude-adjustment using the four reaction wheels are of particular interest from an engineering perspective, and form the core of the technology demonstration programme.

The PROBA project is part of a general move away from the large, resource-intensive, satellites, which have been characteristic of Earth observation over the past 20 years or so; for these missions, the time period between conception and launch is typically much longer than the natural cycle of scientific investigations. Instead, attention is turning to so-called 'smallsats', whose design, build and deployment programme is intended to follow the principles of the 'faster, better, cheaper' initiative, which was introduced by NASA to provide more cost-effective space missions after the failed Mars Lander attempt in 1993 [2]. As a first attempt at implementing this strategy, PROBA has done reasonably well: the time between the initiation of the project and the launch of PROBA-1 was less than four years, and would have been under three years but for delays to the launch caused by factors external to the project.

The first realisation of the PROBA concept, PROBA-1, is a small platform, weighing approximately $100kg$, including payloads, and measuring approximately $60cm \times 60cm \times 80cm$. The spacecraft management (e.g. guidance, navigation and control) is carried out by a high-performance RISC processor; specifically, a space-qualified SPARC V7 device, which provides 10MIPS and 2MFLOPS of processing power. The spacecraft is designed with a nominal lifetime of greater two years. Initially, the intention was to operate PROBA-1 in space for one year only, but the demand for scientific data from the payload instruments has been so great that an extra two years of post-launch support has been funded by ESA.

B. Attitude Control and Pointing

An important element of the on-board autonomy is the control of the spacecraft's attitude. The platform uses GPS instruments (an L1 system with 4 antennae) and star trackers to maintain an accurate record of its position and attitude. The star trackers work by recording an image of deep space, comparing the observed pattern of stars to an internal catalogue of stellar positions. The image processing load is taken by the star tracker itself. This, combined with efficient matching algorithms, mean that the star tracker units impose a very small resource load on the platform itself. The rate of update of the star trackers on-board PROBA-1 is in the range 5–$20Hz$. At $5Hz$, a pointing accuracy of a few arc seconds is achievable.

If just one star tracker is used, it will be blinded periodically by being directed at the moon: the passage of the moon across its field-of-view can last as long as 240 seconds for up to 2 days per month. To avoid this, and to increase the accuracy generally, PROBA-1 employs two star trackers, pointing in different directions. The star trackers are situated to avoid blinding by the sun throughout the duration of the mission, whether as a result of seasonal progression or spacecraft manoeuvring. The additional requirement that they are not blinded by Earth-light limits the across-track pointing of the mission slightly, partly due to the relatively low orbit into which PROBA-1 was eventually placed: it is a minor consideration in a higher orbit.

The spacecraft attitude is controlled by a set of four reaction wheels, which are integrated to the satellite structure. These allow the satellite to be manoevered in each of the three planes (i.e. roll, pitch and yaw). Consequently, the capability to tilt the satellite in both the along-track and across-track directions is a significant feature of the PROBA-1 mission. The maximum rate at which the spacecraft attitude can be varied is approximately $1^\circ s^{-1}$. This is primarily limited by the ability of the star trackers to maintain an accurate register of spacecraft position and attitude, rather than the intrinsic capabilities of the reaction wheels.

As with other missions, such as the HRV and HRVIR sensors on board the SPOT series of satellites, across-track pointing increases the frequency with which a given area of ground is visible to the sensors on-board PROBA-1 [3], and ensures that almost all of Earth's surface is accessible at least once each week. In its present orbit, certain sites are visible to PROBA-1 on two, and occasionally three, successive days. Moreover, by tilting the platform in the along-track direction, its imaging payload is able to acquire a set of up to five images of the same target area during a single overpass.

C. The PROBA Orbit

The PROBA-1 satellite was launched from the Indian Space Research Organisations (ISRO) main launch pad at Shriharikota in India, aboard an ISRO Polar Satellite Launch Vehicle (PSLV). The PROBA-1 orbit is sun-synchronous, with an equatorial crossing time at launch of 10:30. The orbit is somewhat elliptical, with an altitude varying from about $550km$ to about $670km$. This is useful in the context of the PROBA mission, and especially for the space-radiation detection experiment, but is less than optimal for CHRIS activities. In July 2003, the orbital period was 96.77 minutes, the inclination 97.84° and the eccentricity 0.0084. Atmospheric drag makes it impossible to predict more than about two months in advance whether a given site will be visible on a particular day, and the relatively low orbital altitude restricts the across-track pointing, as noted above.

D. Power

Power is provided by Gallium Arsenide solar arrays mounted on five of the six faces of the spacecraft. These provide up to $120W$ peak output and charge the $196Wh$ lithium-ion on-board batteries. In terms of the battery operations, there are four typical operational orbits, these being 'imaging', 'transmission', 'imaging and transmission' and 'quiet'. Orbits where imaging takes place discharge the batteries, while the others charge them; the latter are generally managed autonomously by the on-board mission manager. Any combination of transmission and quiet orbits is allowed, as this leads to a net charging of the on-board battery. Typical image acquisition periods place a higher load on the battery and may increase the Depth of Discharge (DoD) beyond acceptable limits (20% is the acceptable limit, 32% being the maximum recommended). A 'sun-bathing' mode is provided by PROBA, when the maximum possible area of solar panels is exposed toward the Sun during a daytime orbit. The net charge per orbit when sun-bathing is $0.99Ah$. This means that 20% DoD, corresponding to a net charge per orbit of $1.4Ah$, can be completely recovered in two orbits [4].

E. Ground Operations

ESA's ground receiving station at Redu has a $2.5m$ dish, which is dedicated to the PROBA-1 mission. PROBA-1 has 1.2Gbit of on-board data storage located within the Mass Memory Unit (MMU) and its data transfer rates are $4\text{kbit}\,s^{-1}$ for up-link and $1\text{Mbit}\,s^{-1}$ for download. Thus, about 20 minutes are required to download the contents of the MMU in its entirety, equivalent to as many as three overpasses of the Redu ground receiving station. To achieve the greater throughput required to meet the needs of the scientific mission for CHRIS, additional download capacity has been deployed at the Kiruna ground station, while Redu is still used for the data up-link.

III. The CHRIS Instrument

A. General Description

CHRIS is a small hyperspectral imager, designed as a space-borne remote sensing instrument. It consists of a telescope and an imaging spectrometer, attached to a CCD-array detector system. It weighs approximately $14kg$ and occupies a volume of

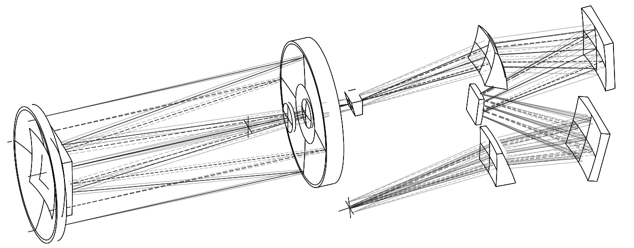

Fig. 1. Optical plan of the CHRIS instrument.

$0.79m \times 0.26m \times 0.20m$. Between the telescope and the spectrometer lies the spectrometer entrance slit, which is treated as part of the telescope assembly in the context of this paper. The telescope forms an image of the distant Earth scene onto the entrance slit, so that the telescope and slit define a slit-shaped instantaneous field-of-view (IFOV). The spectrometer re-images the collected light, disperses it in the direction perpendicular to the slit image, and focuses it on to the area-array detector. The CHRIS deployed on PROBA-1 is limited to channels in the visible and near infra-red wavelengths, but the design allows for an extended range of wavelengths through the use of an additional detector system and minor adjustments to the general instrument layout. The result is a low cost, light weight, instrument with no moving parts, capable of delivering high resolution spectra throughout the visible and near-infra-red wavelengths (400–1050*nm*).

B. Telescope

The telescope has a pupil diameter of 120*mm*, operating at $f/6$, and has a conventional two mirror configuration. After reflection from the primary and secondary mirrors, the beam passes through a central hole in the primary mirror to reach a focus at the entrance slit (Fig. 1). Only spherical surfaces are used. A large meniscus lens at the entrance pupil of the instrument is employed to correct for spherical aberration. This also provides a convenient method for mounting the secondary mirror, which is cemented to the inner face of the meniscus. The telescope optics are completed by two small lenses in the converging beam in the entrance slit assembly, which correct for some minor telescope aberrations and allow the telescope to be approximately telecentric.

The meniscus lens, the secondary to which it is cemented, and the two small lenses are made of fused silica. The primary mirror is made of Schott BK7 glass, to provide a good CTE match to the titanium structure. Lens elements are multi-layer anti-reflection coated to reduce stray reflections below 1.5% per surface at all wavelengths in the nominal instrument range. The telescope mirrors are multi-layer dielectric coated to give 98% reflection per surface over the wavelength range.

The slit is 16.7*mm* long by 0.0255*nm* wide and the focal length of the telescope is 746*mm*, so that at apogee (670*km*) the ground area instantaneously imaged by the slit and telescope is 15*km* across-track by 20*m* along-track; these figures reduce to about 13*km* by 17*m* at perigee.

C. Spectrometer

Light from the slit is dispersed and re-imaged by the spectrometer optics onto the detector, which is an area-array CCD. The spectrometer has a magnification close to 1 for each wavelength in both the along-track and across-track directions (i.e. orthogonal to and parallel to the slit direction, respectively), so that the overall focal length of the combined instrument is the same as that of the telescope (746*mm*). The spectrometer includes two dispersing prisms, so that each point in the entrance slit is re-imaged as a spectrum line, each line being orthogonal to the slit image. Thus, a monochrome image of the entrance slit is formed on each row of detector elements, while the spectrum of each point in the slit (and hence on the ground) is imaged along a detector column.

The re-imaging function of the spectrometer optics is performed by an arrangement of three spherical mirrors. The primary and tertiary mirrors are concave; the secondary is convex. The mirror configuration is very similar to that of a classical Offner relay, with all centres of curvature close together and the radii of curvature of the concave mirrors approximately double that of the secondary. The prisms are placed in the path between the entrance slit and the first mirror, and between the third mirror and the detector. The prism surfaces are spherical to allow correction of their optical aberrations in beams that are diverging and converging.

The prisms are made of fused silica. The mirrors are made of Schott BK7 glass. Again, this is to provide a good CTE match to the titanium structure. With different coatings and minor design adjustments, the system can provide a well-corrected spectrum image for the complete spectral range from UV to 2500*nm*.

The special merits of the spectrometer design are its simplicity, ease of manufacture and alignment, and small dimensions. The simplicity arises from the use of just three mirrors and two refracting elements, which also limits costs and permits good control of out-of-band stray light. The ease of manufacture and alignment are achieved by avoiding aspheric surfaces, difficult materials and optically contacted surfaces. The design is also very compact for the achieved spatial and spectral resolution and relative aperture.

D. CCD

The re-imaged light emerges from the spectrometer with the slit dispersed spectrally, at right angles to the slit direction. The CCD array in the spectrometer focal plane is aligned so that it acquires spatial data in one dimension (columns) and spectral data in the other (rows). The detector used is an e2v CCD-type (CCD25-20), a frame transfer device with 770 columns and 576 rows. It is thinned, back-illuminated and has a single-layer anti-reflection coating, which is uniform over the image area, and quarter-wave effective thickness at 1000*nm*. This gives high quantum efficiency, including good performance in the deep blue spectral region (20% at 400*nm*) and better than 7% at 1000*nm*. The element size is $0.0225mm \times 0.0225mm$. The individual detectors have a dump gate on the output register, which enables rapid dumping of signals from unwanted image areas. The row length of 770 devices provides a useful compromise between the need for a fast line-transfer time and a

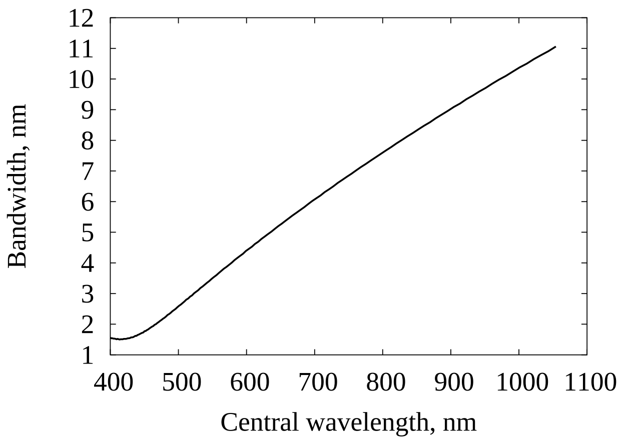

Fig. 2. CHRIS spectral resolution against central wavelength.

wide image swath.

The CCD offers the ability to make radiometric measurements in the spectral range 400–1050*nm* with a spectral resolution that varies from 1.25*nm* to 11.25*nm* across the spectrum (Fig. 2). As has been noted previously, the design of the spectrometer is such that this could be expanded out into the short-wave infrared (up to about 2500*nm*) by the addition of a second detector sensitive to this part of the spectrum. A particular strength of the CCD package is its flexibility in terms of line transfer and read-out. This allows a wide variety of different imaging configurations. These are considered later in this paper. The spectral and spatial definition of any given mode of the CHRIS instrument may, therefore, be controlled by combining or neglecting CCD elements, and by changing the integration time.

E. Theoretical Performance and Tolerances

The telescope gives design resolution better than 0.01*mm* in the focal plane, over the whole spectral range and field of view. Alignment tolerances are generally coarse, so that the spatial resolution is, in practice, limited mainly by the finite sizes of the entrance slit (along track) and the detector pixels (across track). The design performance of the spectrometer optics, in combination with the telescope, is better than 0.012*mm* in the across-track direction, so that spatial resolution is, in theory, limited almost entirely by the finite detector element size (0.0225*mm*). The design resolution of the spectrometer is better than 0.011*mm* in the spectral-dispersion direction for most of the wavelength range, so that, in practice, the spectral resolution is similarly limited mainly by the dimensions of the slit and detectors. The half-width of the instrument line-spread functions in the column direction is approximately 0.0255*mm* (i.e. one detector width), although charge dispersion in the detector degrades this slightly at near infrared wavelengths. Spectral resolution varies with wavelength, following the typical dispersion provided by refraction through fused silica prisms. The theoretical half-width of the line-spread functions correspond to spectral resolutions of 1.25*nm* at 415*nm*, increasing to 11.25*nm* at 1050*nm* (Fig. 2).

The complete optical design is optimised so that monochromatic images of the slit fall on straight detector rows, and line spectra of resolved ground areas fall on detector columns. Departures from these two conditions are known, respectively, as 'smile' and 'frown'. In design, the worst case smile, in terms of wavelength errors, is 0.00035*mm* at 1050*nm*, corresponding to a wavelength error of 0.2*nm*. The worst-case frown is 1% of the pixel width.

F. Stray Light Control

The low-cost telescope design presents some interesting challenges in terms of stray-light control. The main source of stray-light error is believed to be produced by low-angle scatter at optical surfaces, arising from imperfections in the polish and coatings. In particular, some light from the scene can reach the entrance slit by transmission through the three lens elements, without reflection at either mirror. An over-sized secondary mirror, and a sequence of baffles are deployed to mitigate these possibilities. An analysis of stray-light for the instrument confirms the expectations from the optical design, namely that radiance errors equivalent to 0.5% of the average scene radiance are achievable.

IV. CHRIS ON PROBA: MISSION CHARACTERISTICS

The combination of a programmable imaging spectrometer (CHRIS) and an agile, pointable, satellite platform (PROBA-1) offers considerable flexibility in terms of image data acquisition. As a result, it is possible to tailor the data acquired by PROBA/CHRIS to address the particular needs of selected science problems. More specifically, the CHRIS instrument on board PROBA-1 offers some control over the spatial resolution of the image data (by a factor 2), the number and spectral bandwidths of the wavebands in which these data are recorded, and the view zenith and azimuth angles at which they are acquired. In practice, given that this is primarily an experimental mission, a single mode of angular sampling is employed, and the spectral and spatial sampling options (i.e. those realised by particular on-chip averaging configurations) are limited to a few operational modes for almost all acquisitions.

A. Sampling Characteristics

The spatial sampling characteristics (17*m* or 34*m* nominal sampling interval and 13*km* nominal swath) have already been outlined. The main purpose of having the coarser spatial resolution is to increase the number of bands that can be read out from the CCD array. Thus, there is a trade-off between spatial and spectral resolution. A half-swath option at full spatial resolution is another of the operational modes; this again trades some spatial information for enhanced spectral information. In theory, it is also possible to accept the coarser spatial resolution over the half-swath, giving just 190 or so pixels across-track, to increase the number of spectral bands still further (over 100, in fact). The spatial sampling interval varies by ±8% around the orbit, and in time at any one location, because of the varying altitude of the satellite.

A.1 Spectral Sampling

In practice, the operational modes of CHRIS are characterised in terms of different combinations of spatial resolution, swath

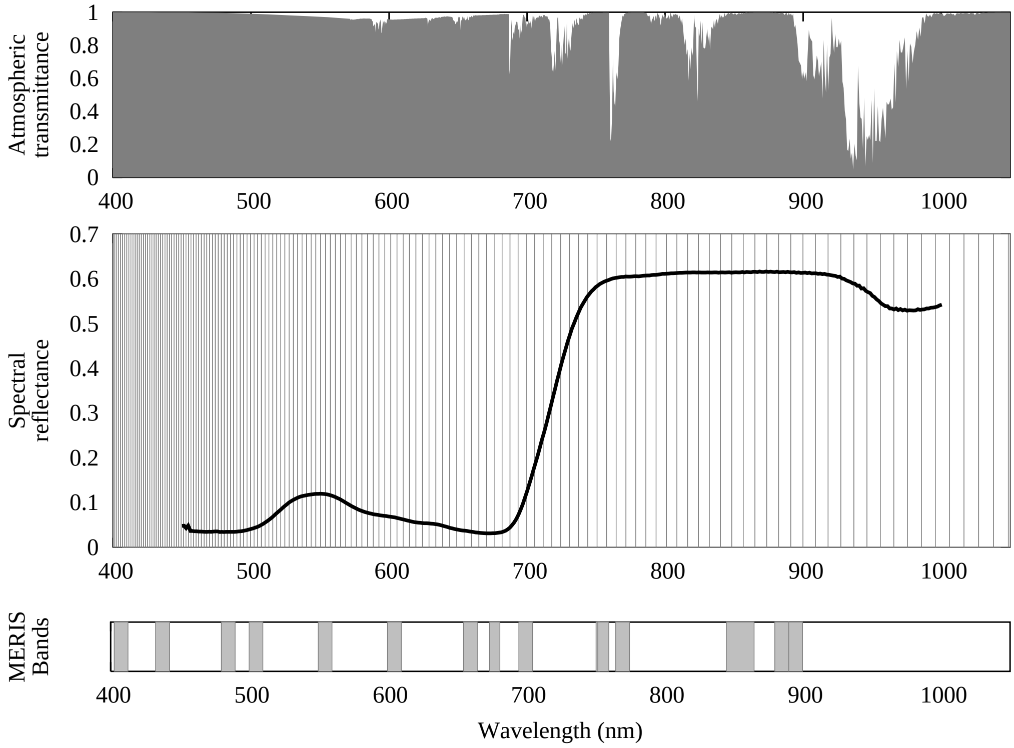

Fig. 3. CHRIS Mode 1 Band Set (62 spectral channels) compared with the nominal atmospheric transmittance (top), the spectral reflectance of vegetation (middle; solid line) and MERIS spectral bands (bottom).

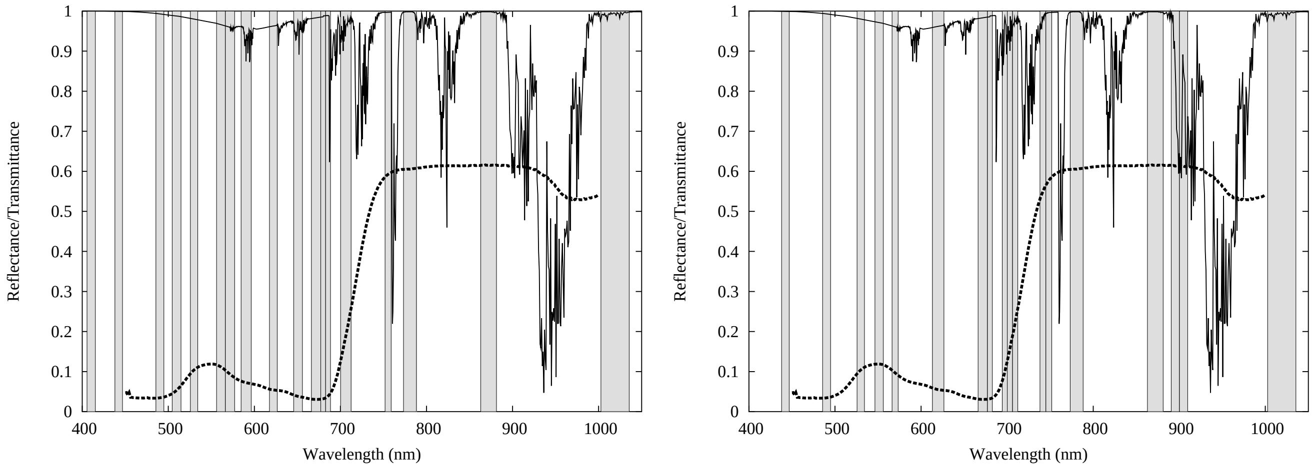

(a) Mode 2 Band Set (Water)

(b) Mode 3 Band Set (Land/Aerosols)

Fig. 4. CHRIS Mode 2 (Water) and 3 (Land/Aerosols) band sets, with typical atmospheric transmittance (continuous line) and vegetation spectral reflectance (dashed line) curves superimposed.

width and spectral band sets, as outlined below. Other modes have been used for specific tasks such as wavelength calibration.

A.1.a *Mode 1: Full Swath, Reduced Spatial Resolution*. In this mode, CHRIS acquires image data across a full swath (nominal 13*km*) at reduced spatial resolution (nominal 34*m*), in 62 spectral channels (Fig. 3). Most channels are 5–10*nm* wide, and the set is largely contiguous.

A.1.b *Modes 2–4: Full Swath, Full Spatial Resolution*. This is the most common mode of operation, in which CHRIS is used to acquire image data at the highest spatial resolution (nominal 17*m*) over the full swath and in 18 spectral channels. The latter are obtained by binning the signals from sets of CCD rows, allowing the bands to be selected anywhere in the instrument's spectral range. In this mode, three standard spectral band sets have been defined. These are intended for studies of water bodies (Mode 2; Fig. 4(a)), the land surface and atmospheric aerosols (Mode 3; Fig. 4(b)), and chlorophyll (Mode 4). Where this can also be satisfied, the standard bands sets have been configured to permit inter-comparisons with other satellite sensors, such as MODIS and MERIS. In any case, the convergence of interest in a similar set of science problem lead us to locate the CHRIS bands at similar wavelengths to those chosen for other satellites.

A.1.c *Mode 5: Half Swath, Full Spatial Resolution*. CHRIS can also be used to acquire image data across half of the nominal swath at the highest nominal spatial resolution. In this mode, the instrument is able to record image data in 37 spectral channels.

A.2 Angular Sampling

As was noted earlier, the PROBA-1 satellite can be manoeuvred in all three axes to view any target of interest, which is very important for an instrument with a small image swath, such as this, and only sites at the very highest latitudes are inaccessible to the mission. More significantly, by tilting PROBA-1 in both the along-track and across-track directions during orbit, it is possible to acquire a set of up to five CHRIS images of a given target area, each at a different view zenith angle, in a single data acquisition sequence; that is, during a single orbital overpass (see, for example, Fig. 5). It is important to realise that the CHRIS instrument is only occasionally able to image a target area from directly overhead (i.e. in nadir-viewing mode) because of its relatively narrow field-of-view. More generally, PROBA-1 must be tilted at some angle in the across-track direction so that the target area falls within the sensor's field-of-view. Each target site therefore has an associated 'fly-by position' on any given day; this is the point on the sub-satellite track that is closest to the target. The platform acquires images of the target when the zenith angle of the platform, *with respect to the fly-by position*, is one of the following: $\pm 55°$, $\pm 36°$ and $0°$. The zenith angles with respect to the target will typically be somewhat larger than these values, especially for the 'nadir' images. In practice, this means that the angles at which images are acquired vary from site-to-site, depending on their positions with respect to the orbital track. By comparison, the view zenith angles at which the MISR cameras acquire image data are, to the nearest degree, $\pm 70°$, $\pm 60°$, $\pm 46°$, $\pm 26°$ and nadir [5], while the Along Track Scanning Radiometer series (ATSR, ATSR-2 and AATSR) have dual-view capability, with data recorded at nadir (actually, between $0°$ and $20°$) and at $55°$ [6], [7].

TABLE I
PROBA/CHRIS IMAGING SEQUENCE.

Tag Number	FZA	Scan Direction
3	$+55°$	N–S
1	$+36°$	S–N
0	$0°$	N–S
2	$-36°$	S–N
4	$-55°$	N–S

In the context of the PROBA/CHRIS mission, the view zenith angle of the satellite at the fly-by position is known as the Minimum Zenith Angle (MZA). The convention adopted is that this angle is reported as a negative number when the target lies to the east of the sub-satellite track, and positive when it lies to the west. The scan direction in which the five images are acquired alternates, to minimise the slewing required between images, and each image is assigned a unique tag number (Table I).

A.3 Temporal Sampling

It is possible to take still further advantage of the across-track pointing of PROBA-1, to acquire up to three separate sets of multiple-view-angle CHRIS images with respect to a given target area, each from a different orbital overpass, over the period of several days. The opportunities for repeated imaging of a target are determined by its latitude and a factor related to the immediate properties of the orbit. At the equator, any point can be imaged by CHRIS once every seven to eight days. If the overpass has a small MZA, this will be the only chance to image the site but, if the MZA is larger, the site may be visible on two successive days. At higher latitudes, the opportunities for imaging on two successive days increases and, if the satellite is close to apogee, it is possible that the site will be visible to PROBA/CHRIS on three successive days — one view will be from the east, one from the west, and one from an overpass with a relatively small ($<5°$) MZA. The different sensor viewing angles and, to a lesser extent, the small changes in solar zenith angle at which these images are acquired enable PROBA/CHRIS to sample the BRDF of the target surface. For example, on the 12^{th}, 13^{th} and 14^{th} of July 2003, the community site at Barrax, Spain (latitude $39°N$) was visible to PROBA/CHRIS with MZAs of $20°$, $-4°$ and $-27°$, respectively. The pattern with which any site is accessible to the platform varies at roughly eight-day intervals, but with some shifting in MZA, because the orbit does not repeat exactly. For example, Barrax was visible for just two successive days a week later (MZA $15°$ and $-9°$ on the 20^{th} and 21^{st}, respectively).

B. Mission Science

Reflectance from Earth's surface is almost always anisotropic. As a result, a measurement of surface reflectance acquired at a single sensor view angle has only limited usefulness in terms of estimating the surface albedo, which is a critically important parameter of the surface radiation budget and, hence, the surface energy budget [8], [9]. The directional reflectance properties

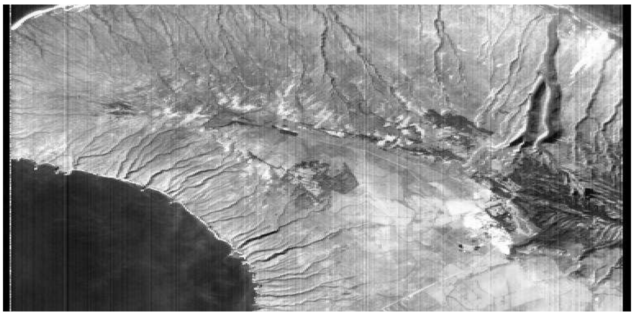

(a) −55°

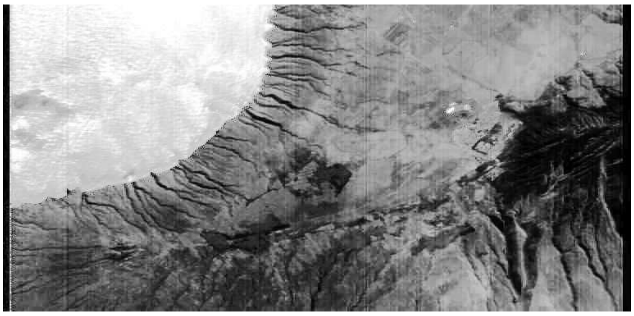

(b) −36°

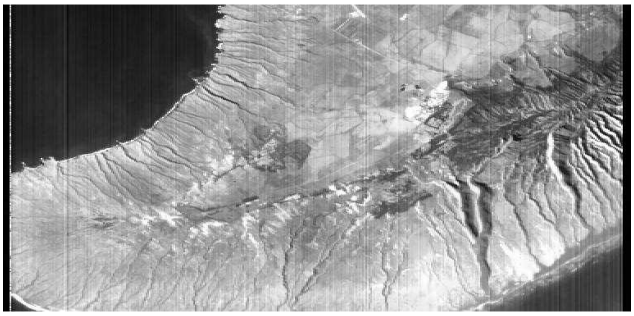

(c) +36°

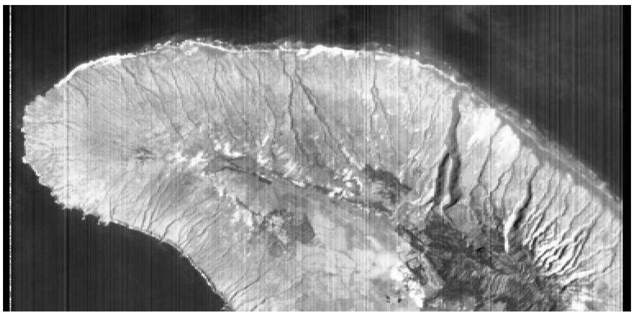

(d) +55°

Fig. 5. Four single-band images from a multiple-view-angle set acquired by PROBA/CHRIS over Lana'i, one of the Hawaiian islands, on December 6, 2002.

of Earth's surface also mean that a comparison of reflectance measurements made at two different times (e.g. for change detection purposes) is likely to be compromised, if variations in reflectance with viewing geometry are not taken into account. Thus, the proper interpretation of a measurement made at a single view angle often requires an understanding of the directional reflectance properties of the surface; simple spectral discrimination of different cover types is perhaps the only exception, although even here a set of directional-spectral measurements can help to improve the separability of different vegetation types, when compared to a single multispectral image [10].

At the risk of over-simplification, one might argue that spectral variation in reflectance is largely determined by the chemical composition of the surface materials, while angular variation is determined their structural properties [11]. One of the main contributions of the PROBA/CHRIS mission, therefore, will be the validation of surface reflectance models, at spatial scales that can be tied to simultaneous ground measurements of canopy variables [12].

The atmosphere also reflects light non-isotropically. Scattering by permanent gases is well characterised by theory and it is relatively simple to account for this contribution to the top-of-atmosphere signal. Scattering by optically active aerosols is more problematic. This has a strong forward-scattering component, but the precise phase function depends on the size distribution of the particles present. Again, as for the land, the directional quality of the atmospheric reflectance distribution carries information on the causes of the anisotropy, and multi-view data have been used to estimate concentrations of optically active aerosols [7], [13].

The initial plan for the data from CHRIS was designed to exploit the multiple-view-angle capabilities of the instrument to retrieve either atmospheric aerosol properties or land-surface geophysical properties related to the BRDF. In each case, the intention was, initially at least, to collect data over a limited number of well-characterised and instrumented sites (e.g. Aeronet sites in the case of aerosols and selected MODIS MODLAND Cal/Val sites for the surface properties). Coastal studies were later added, since the CHRIS instrument shares some heritage in design terms with the MERIS sensor, and a decision was therefore made to broaden the scientific user base. It was subsequently decided to open up the mission to a still wider scientific audience by means of an Announcement of Opportunity, which was issued by ESA in 1999. As a result, there are now some 60 locations on the list of scientific sites for which CHRIS acquires images, and these have been partly prioritised. The mission now includes a number of sites for the study of coastal and inland waters, and a wider range of land applications including forestry, agriculture and surface energy budgets. Some of these exploit the programmability of the CHRIS to select different sets of spectral channels for specific applications.

B.1 Land-Surface Studies

Models of the BRDF for vegetation canopies show that the varying intensity in reflected radiance is determined principally by structural features, such as gaps and the arrangement, orientation and spacing of the surface-scattering elements (e.g. leaves, stems and branches) [14]. The more parsimonious models of

BRDF allow most of the surface reflection, aside from the ‘hot-spot’, to be captured in terms of a few parameters. Characterisation of the surface in terms of an appropriate BRDF model enables robust, physically based relationships between albedo and directional radiance to be developed, but the validation of these models over large areas is difficult. In this context, the directional data from PROBA/CHRIS will be used both for the validation and refinement of top-of-canopy BRDF models, and for the retrieval of geophysical parameters, such as leaf area index and canopy chlorophyll content, by inversion of simplified versions of those models, or through the use of look-up table (LUT) approaches applied to more sophisticated models [12]. This original theme is now joined by a range of land surface studies, including the assimilation of CHRIS data into models of plant growth, as well as more conventional red-edge position (REP) investigations and land cover studies. In many cases, simultaneous measurements of surface reflectance and atmospheric optical properties are needed to validate the CHRIS data and the derived products, so that dedicated fieldwork is required, although automatically instrumented sites have also been included.

B.2 Atmospheric Aerosols

Aerosols (liquid droplets and atmospheric particulate matter) are an important radiative constituent of the atmosphere, with sulphate aerosols in particular able to reflect significant amounts of energy back to space. Apart from their direct radiative forcing effect, aerosols have an indirect effect through their role as cloud condensation nuclei, although the interaction between clouds and aerosols is a complex story with many uncertainties. Little is known about global aerosol distribution, and how it varies in time, although this is being rectified with the expansion of the Aeronet system [15] and the continuous delivery of global aerosol products from instrument such as MISR [5].

MVA data can be used to estimate aerosol properties under appropriate directional sampling conditions [16], [17], which was the rationale behind the nine-view MISR instrument [18], [19], [5]. Nine viewing directions may not always be needed; the ATSR2 instrument [20] combines just two views of the ground in four solar channels, but this has been found adequate for good estimates of aerosol optical depth [21], [22], [7], [23]. In comparison with the existing MVA instruments, which have just a few spectral channels, the CHRIS allows an almost continuous spectrum to be obtained at high spectral resolution ($\sim 10nm$), and it is hoped the extra spectral information will allow inferences to be made about the particle size distribution of the aerosols.

Existing MVA satellite-borne instruments tend to have large footprints — 2–4*km* in the case of ATSR2, about 14*km* in the case of POLDER [24], [25], and roughly 20*km* in terms of the global aerosol product delivered by MISR. The dangers of scaling errors in such retrievals may be real, given that aerosol concentration can vary significantly over smaller lengths scales, especially in the vicinity of aerosol sources. The high spatial resolution of the CHRIS may allow any such scaling effect to be characterised. Perhaps more importantly, the retrievals from CHRIS are at a scale between the point measurements of the Aeronet network, and the multiple-kilometre areas covered by AATSR and MISR pixels, and should make possible a more sensible validation of the latter with the former. At some, non-Aeronet sites, ground-based lidars will be deployed as part of the PROBA/CHRIS programme to obtain vertical profiles of aerosol distributions.

B.3 Coastal and Inland Waters

The remote sensing of coastal and inland waters requires sensors with a high spatial resolution and the ability to provide multi-temporal imagery. Cracknell has argued that Earth observation has been far less successful in the shallow coastal zone compared to the deep ocean and atmosphere, in part because limited scanner resolution and image frequency have prevented observation of the relevant scales in shelf seas and estuaries [26]. PROBA/CHRIS provides a higher spatial resolution than existing ocean colour sensors (MERIS currently has the highest spatial resolution, which is 300*m*). The critical question will be whether PROBA/CHRIS has the required radiometric sensitivity to map not just suspended particulate matter, but also phytoplankton, since it was not originally designed to act a sensor for the marine environment.

CHRIS is being used over a small number of coastal and inland water sites in Europe. The core test sites are well characterised and represent a range of Case II waters (dominated by sediment or coloured dissolved organic matter), although some of which on occasion are more similar to Case I (phytoplankton dominated) waters. Wherever possible, the sites and acquisitions are chosen to augment existing, pre-planned, campaigns with research ship support. Most sites have *in situ* sampling (both optical and bio-geochemical) during the CHRIS acquisition periods, sun photometer (atmospheric) measurements and other forms of remote sensing (additional airborne/satellite systems). Accurate atmospheric correction is very important to these studies, as the water-leaving signal represents a small contribution to the top-of-the-atmosphere value. The main contribution of the directional component of the data, here, is to make possible a more accurate atmospheric correction.

C. Acquisition Planning/Schedule : Ground Segment

In keeping with the experimental nature of the overall mission, the ground segment for the scientific component is relatively modest. There is a steering committee for the CHRIS instrument, which considers requests for scientific acquisitions and which has developed a simple scheme for prioritising data acquisitions among the different sites and users, with the aim of maximising the acquisition of useful data. Highest priority tends to be given to experiments where large ground-campaigns are taking place simultaneous to the CHRIS overpasses, particularly those involving, for example, ship-time or the deployment of ground-based lidars, or similar equipment, away from their usual base. Investigations where angular sampling is an important element of the science are preferred to those that are interested merely in hyperspectral data; similarly, instrumented sites are preferred to non-instrumented ones. Perhaps the strongest determinant of all, however, is weather. A prioritised short-list of candidate sites is compiled for each day, a week or so in advance, but the choice of which image to take on any given day rests on the expected cloud cover for each site, based on predictions obtained from the UK MetOffice. For major campaigns, the image is taken even if the likelihood of overcast conditions is greater than 50%, but for remotely-instrumented sites, such as Aeronet locations, a threshold (10%) of acceptable cloud cover is imposed. This experience of scheduling is expected to be very useful material in terms of planning SPECTRA and other follow-on missions to PROBA/CHRIS.

V. Summary

The PROBA platform is one of the first products arising from a new and increasingly influential philosophy within the European Space Agency and the British National Space Centre, following a NASA lead. To ensure that satellite-based Earth observation missions can be delivered in a time-frame that makes their data useful to scientists, missions need to become more tightly focused, and the time taken from the original concept to launch and operation must be greatly reduced, if the necessary responsiveness is to be realised. The mission considered here has managed to put an imaging spectrometer (CHRIS) into Earth orbit in a little under three years, notwithstanding a long delayed launch, for a cost of about 10 million US dollars, or Euros. The mission is about more than showing how quickly something can be put into space, however. Innovative design in both the platform and spectrometer have also been pursued successfully and, although the data from the CHRIS will not, strictly, answer focused science questions that can only be addressed through the use of a pointable imaging spectrometer, the highly resolved, multi-view, hyperspectral datasets that it generates are providing a rich source of data that will take several years to analyse, and that is already helping to shape the related missions that are to follow.

Acknowledgements

MJB would like to acknowledge the support of the UK Natural Environment Research Council, through grant number NER/Z/S/1999/00130. Thanks are also due to Dr. P. Lewis, Dr. T. Quaife and Dr. G. Thackrah at University College London for their help and advice in connection with the PROBA/CHRIS project. The image data presented in this paper are derived from the CHRIS instrument, developed by Sira Technology Ltd (formerly Sira Electro-Optics Ltd), with support from the British National Space Centre, mounted on board the European Space Agency's PROBA-1 platform.

References

[1] M. J. Barnsley, "Environmental monitoring using multiple-view-angle (mva) remotely-sensed data," in *Environmental remote sensing from global to regional scales* (G. M. Foody and P. J. Curran, eds.), pp. 181–201, Chichester: John Wiley and Sons, 1994.

[2] H. E. McCurdy, *Faster, Better, Cheaper*. Boston, USA: Johns Hopkins University Press, 2001.

[3] M. J. Barnsley, K. P. Morris, A. H. Strahler, and J.-P. Muller, "Sampling the surface bidirectional reflectance distribution function (brdf): Evaluation of current and future satellite sensors," *Remote Sensing Reviews*, vol. 8, pp. 893–916, 1994.

[4] P. van den Braembussche, L. Dayers, D. Rosseneu, and J. Bermyn, "Proba mission analysis," Tech. Rep. PROBA-TN-080-VE, ESA, Noordwijk, Netherlands, 1999.

[5] D. J. Diner, J. C. Beckert, T. H. Reilly, T. P. Ackerman, C. J. Bruegge, J. E. Conel, R. Davies, S. A. W. Gerstl, H. R. Gordon, R. A. Kahn, J. V. Martonchik, J.-P. Muller, R. Myneni, B. Pinty, P. J. Sellers, and M. M. Verstraete, "Multi-angle imaging spectroradiometer (misr): instrument description and experiment overview," *IEEE Transactions on Geoscience and Remote Sensing*, vol. 36, no. 4, pp. 1500–1530, 1998.

[6] C. Godsalve, "Bidirectional reflectance sampling by atsr-2 - a combined orbit and scan model," *International Journal of Remote Sensing*, vol. 16, no. 2, pp. 269–300, 1995.

[7] P. North, S. Briggs, S. Plummer, and J. Settle, "Retrieval of land surface bidirectional reflectance and aerosol opacity from atsr-2 multi-angle imagery," *IEEE Transactions on Geoscience and Remote Sensing*, vol. 37, no. 1, pp. 526–537, 1999.

[8] D. S. Kimes, P. J. Sellers, and D. J. Diner, "Extraction of spectral hemispherical reflectance (albedo) of surfaces from nadir and directional reflectance data," *International Journal of Remote Sensing*, vol. 8, pp. 1727–1746, 1987.

[9] M. J. Barnsley, P. Lewis, M. Sutherland, and J. Muller, "Estimating land surface albedo in the HAPEX-Sahel southern super- site: inversion of two BRDF models against multiple angle ASAS images," *Journal of Hydrology*, vol. 189, no. 1-4, pp. 749–778, 1997.

[10] A. H. Hyman and M. J. Barnsley, "On the potential for land cover mapping from multiple-view-angle (mva) remotely-sensed images," *International Journal of Remote Sensing*, vol. 18, no. 11, pp. 2471–2475, 1997.

[11] M. J. Barnsley, D. Allison, and P. Lewis, "On the information content of multiple view angle (mva) images," *International Journal of Remote Sensing*, vol. 18, no. 9, pp. 1937–1960, 1997.

[12] M. Barnsley, P. Lewis, S. O'Dwyer, M. Disney, P. Hobson, M. Cutter, and D. Lobb, "On the potential of chris/proba for estimating vegetation canopy properties from space," *Remote Sensing Reviews*, vol. 19, pp. 171–189, 2000.

[13] P. R. J. North, "Estimation of aerosol opacity and land surface bidirectional reflectance from atsr-2 dual-angle imagery: operational method and validation," *Journal of Geophysical Research*, vol. 107 (D12), no. 4149, 2002.

[14] N. S. Goel, "Models of vegetation canopy reflectance and their use in the estimation of biophysical parameters from reflectance data," *Remote Sensing Reviews*, vol. 3, pp. 1–212, 1987.

[15] B. N. Holben, T. F. Eck, I. Slutsker, D. Tanré, J. P. Buis, A. Setzer, E. Vermote, J. A. Reagan, Y. J. Kaufman, T. Nakajima, T. Lavenu, I. Jankowiak, and A. Smirnov, "Aeronet — a federated instrument network and data archive for aerosol characterization," *Remote Sensing of Environment*, vol. 66, no. 1, pp. 1–16, 1998.

[16] J. V. Martonchik and D. J. Diner, "Retrieval of aerosol and land surface optical properties from multi-angle satellite imagery," *IEEE Transactions on Geoscience and Remote Sensing*, vol. 30, pp. 223–230, 1992.

[17] J. V. Martonchik, D. J. Diner, R. A. Kahn, T. P. Ackerman, M. M. Verstraete, B. Pinty, and H. R. Gordon, "Techniques for the retrieval of aerosol properties over land and ocean using multiangle imaging," *IEEE Geoscience and Remote Sensing*, vol. 36, pp. 1212–1227, 1998.

[18] D. J. Diner, C. J. Bruegge, J. V. Martonchik, T. P. Ackerman, R. Davies, S. A. W. Gerstl, H. R. Gordon, P. J. Sellers, J. Clark, J. A. Daniels, E. D. Danielson, V. G. Duval, K. P. Klaasen, G. W. Lilienthal, D. I. Nakamoto, R. J. Pagano, and T. H. Reilly, "Misr: A multiangle imaging spectroradiometer for geophysical and climatological research from eos," *IEEE Transactions on Geoscience and Remote Sensing*, vol. 27, pp. 200–214, 1989.

[19] D. J. Diner, C. J. Bruegge, J. V. Martonchik, G. W. Bothwell, E. D. Danielson, V. G. Ford, L. E. Hovland, K. L. Jones, and M. L. White, "A multiangle image spectroradiometer for terrestrial remote sensing with the earth observing system," *International Journal of Imaging Systems and Technology*, vol. 3, pp. 92–107, 1991.

[20] A. J. Prata, R. P. Cechet, I. J. Barton, and D. T. Llewellyn-Jones, "The along-track scanning radiometer for ers-1 : Scan geometry and data simulation," *IEEE Transactions on Geoscience and Remote Sensing*, vol. 28, pp. 3–13, 1990.

[21] R. J. Flowedew and J. D. Haigh, "Retrieval of aerosol optical thickness over land using the ATSR-2 dual look satellite radiometer," *Geophysical Research Letters*, vol. 23, pp. 351–354, 1996.

[22] G. Mackay, M. D. Steven, and J. A. Clark, "An atmospheric correction procedure for the ATSR-2 visible and near-infrared land surface data," *International Journal of Remote Sensing*, vol. 19, pp. 2949–2968, 1998.

[23] P. North, "Estimation of fapar, lai, and vegetation fractional cover from atsr-2 imagery," *Remote sensing of Environment*, vol. 80, pp. 114–121, 2002.

[24] P.-Y. Deschamps, F. M. Bréon, M. Leroy, A. Podaire, A. Bricaud, J. C. Buriez, and G. Seze, "The polder mission — instrument characteristics and scientific objectives," *IEEE Transactions on Geoscience and Remote Sensing*, vol. 32, no. 3, pp. 598–615, 1994.

[25] M. Leroy, J. L. Deuze, F. M. Breon, O. Hautecoeur, M. Herman, J. C. Buriez, D. Tanre, S. Bouffies, P. Chazette, and J. L. Roujean, "Retrieval

of atmospheric properties and surface bidirectional reflectances over land from polder/adeos," *Journal of Geophysical Research-Atmospheres*, vol. 102, no. D14, pp. 17023–17037, 1997.

[26] A. P. Cracknell, "Remote sensing techniques in estuaries and coastal zones — an update," *International Journal of Remote Sensing*, vol. 20, pp. 485–496, 1999.

Michael J. Barnsley is Research Professor of Remote Sensing and Head of Department in the Department of Geography, University of Wales Swansea, Singleton Park, Swansea SA2 8PP, UK. He is Director of the NERC Climate and Land-Surface Systems Interaction Centre (CLASSIC), based at Swansea.

Jeff Settle is Senior Research Fellow in the NERC Environmental Systems Science Centre, University of Reading, UK. He holds a MA from the University of Cambridge, UK and a PhD from the University of London, UK.

Mike Cutter is Business Director for Space at Sira Technology Ltd, part of the Sira Group of companies, based in Chislehurst, Kent, UK.

Dan Lobb is the Senior Systems Engineer at Sira Technology Ltd, part of the Sira Group of companies, based in Chislehurst, Kent, UK.

Frederic Teston is the PROBA Project Manager at ESA. He is currently based at ESA/ESTEC, Noordwijk, The Netherlands.